CORE
Metadata, citation and similar papers at core.ac.uk
Provided by Digital.CSIC

Plasma diagnostics and device properties of AlGaN/GaN HEMT passivated with SiN deposited by plasma enhanced chemical vapour deposition (PECVD).

M. F. Romero,[1] M. M. Sanz,[1] I. Tanarro,[2] A. Jiménez[3] and E. Muñoz[1]*

[1]ISOM-Univ. Politécnica de Madrid (UPM). ETSIT, Madrid, Spain.

[2]Inst. de Estructura de la Materia, CSIC, Madrid, Spain

[3]Dpto. Electrónica, Escuela Politécnica Superior, Univ. de Alcalá, Alcalá de Henares, Madrid, Spain

**Corresponding author: itanarro@iem.cfmac.csic.es*

Key words: High Electron Mobility Transistors (HEMT), AlGaN/GaN, silicon nitride (SiN) thin films, SiH_4 - NH_3 plasmas, plasma diagnostics, plasma enhanced chemical vapour deposition (PECVD).

Abstract

In this work, silicon nitride thin films have been deposited by Plasma Enhanced Chemical Vapour Deposition (PECVD) on both silicon samples and AlGaN/GaN High Electron Mobility Transistors (HEMT) grown on sapphire substrates. Commercial parallel-plate RF plasma equipment has been used. During depositions, the dissociation rates of SiH_4 and NH_3 precursors and the formation of H_2 and N_2 have been analysed by mass spectrometry as a function of the NH_3/SiH_4 flow ratio and the RF power applied to the plasma reactor. Afterwards, the properties of the films and the HEMT electrical characteristics have been studied. Plasma composition has been correlated with the SiN deposition rate, refractive index, H content and the final electric characteristics of the passivated transistors.

1. Introduction

Silicon nitride (SiN) thin films deposited by PECVD are widely used in the semiconductor industry as passivating layer [1-3], diffusion barrier [4], gate dielectric [5,6] or interlevel metal isolation. They are also currently employed as antireflection and protective coatings in solar cells [7,8], and have been investigated to fabricate membranes for micromechanical applications [9]. Silicon nitride can also be deposited by thermal CVD or catalytic CVD [10], but plasma enhancement renders uniform deposition over large areas and allows the use of much lower substrate temperatures [6], compatible with most of the steps in semiconductor processing.

At present, SiN thin films are increasingly used as passivating coatings of AlGaN/GaN High Electron Mobility Transistors (HEMT), which have proved to be excellent candidates for high-power and high-temperature requirements [11], from DC to high frequencies [12-14], owing to the great thermal stability, large band offsets and high spontaneous and piezoelectric fields of the nitrides. These field effect transistors, which incorporate a junction between two materials with different band gaps, based on AlGaN/GaN heterostructures, provide huge sheet-carrier densities ($\sim 10^{13}$ cm^{-2}), even for temperatures above 1000 K [15]. Nevertheless, the advantages of nitride-based devices are hindered by the large defect density of this material. So, AlGaN/GaN HEMT exhibit the instability phenomenon of current collapse, which seems to be related to surface effects [16]. Recently, it has been shown that the HEMT processing and, in particular, the SiN passivation process, have noticeable effects on minimizing current collapse and achieving a suitable passivation of these devices [17,18]. By this reason, a complete characterization of the SiN passivation process is desirable.

Plasma diagnostic, allowing to identify transient species, as well as stable products and other properties involved in plasma processing, has become a powerful method to understand the mechanisms which ultimately lead to the growth of films of the most diverse characteristics [19-21]. The diagnostic is mainly carried out with spectroscopic techniques like visible emission of excited species [6,22-25] or infrared absorption of molecular bands [7,26-30]; by mass spectrometry of neutrals [1-3,6,31,32] and ions [33-35], and with Langmuir probes [36,37]. Many of these studies are usually performed on experimental plasma reactors, specially designed to allow the use of some of the former characterization techniques. Nevertheless, in commercial equipments, devoted specifically to optimize thin film production, the plasma diagnostic capabilities are often very restricted. The results found in experimental reactors cannot be always extrapolated directly to the commercial ones. Even the conditioning of the reactor surfaces with previous plasma treatments can influence the subsequent film properties [18]. Therefore, attempts for *in-situ* characterizing the plasmas generated in this kind of reactors during film processing are worthwhile, since they can be of great help to guide the improvement

of the deposition processes and the quality of the films [38].

In order to produce SiN thin films by PECVD, gas mixtures of SiH_4 + NH_3 or SiH_4 + N_2 are commonly used. The composition of SiH_4 + NH_3 and SiH_4 + N_2 depositing plasmas under different conditions, and its influence on the properties of SiN films, have been studied by some authors in various types of reactors, always looking for an optimization of the characteristics of the films, depending on their further applications. The deposited SiN films do not consist of stoichiometric Si_3N_4 crystals, but are more properly described as amorphous $Si_xN_yH_z$. The hydrogen content, which is determinant in the film characteristics, is higher when NH_3 is used as precursor. Nevertheless, this molecule can be dissociated much more efficiently at electron energies remarkably lower than those needed to dissociate N_2 [3,6] and therefore is more widely used. To drive out the excess of hydrogen, substrate temperatures ~300 ºC or higher are usually employed during deposition processes.

Smith and co-workers [1-3] studied SiH_4 + NH_3 and SiH_4 + N_2 plasmas generated in a parallel plate RF plasma reactor; characterized the plasmas by means of line-of-sight mass spectrometry, and studied the plasma composition for various plasma powers and gas mixture conditions, with the aim of minimizing the rate of charge trapping in Al/$Si_xN_yH_z$/Si Metal-Insulating-Semiconductor (MIS) capacitors. They also found that in the case of SiH_4 + NH_3 plasmas, the main deposition precursor was the triaminosilane ($Si(NH_2)_3$) radical [1], whereas in the case of SiH_4 + N_2 plasmas, SiH_n radicals and N atoms react directly at the substrate surface [2]. Kessels *et al* [26] confirmed and refined these last results after measuring by laser absorption spectroscopy and mass spectrometry the densities of SiH_3 and N in a SiH_4 + N_2 expanding thermal plasma, which was used to deposit SiN films at high deposition rates (>1 nm/s) for photovoltaic applications [7]. Oever *et al* [27] employed cavity ring-down absorption spectroscopy and threshold ionization mass spectrometry for the diagnostic of N, NH, and NH_2 radical densities in a remote Ar–NH_3–SiH_4 expanding thermal plasma and inferred the possible role of these transients in silicon nitride deposition. Ohta *et al* [33] studied by mass spectrometry the influence of ions like NH_4^+ on the growth of ultra-thin SiN films in SiH_4 + NH_3 electron cyclotron resonance plasmas, devoted to produce gate dielectric films in large scale integrated circuits. Flewitt *et al* [6] succeed in depositing SiN films with low H content at low temperature (80 ºC) using SiH_4 + N_2 + He electron cyclotron resonance plasmas, which would allow the use of plastic instead of glass substrates for liquid crystal displays, and inferred the relevance of gas phase reactions. So, in the previous studies, the main deposition mechanisms of silicon nitrides were quite thoroughly elucidated, and it was demonstrated that the plasma chemistry can be manipulated to control the film properties in a reproducible and predictable manner.

In this work, SiN thin films have been deposited on silicon samples (to test the film properties) and on High Electron Mobility Transistors (HEMT) previously processed on

AlGaN/GaN heterostructures grown on sapphire substrates [39]. To deposit the films, a commercial RF parallel-plate PECVD reactor has been used, and different NH_3/SiH_4 flow ratios ($\Phi NH_3/\Phi SiH_4$) and RF discharge powers (P_{RF}) have been tested. The dissociation of the precursors and the formation of hydrogen in the plasma have been observed *in situ* by mass spectrometry, and the properties of the films and of the HEMT have been characterized later. A high correlation has been found between the plasma composition under the different deposition conditions and the subsequent properties of the films and the HEMT. The data are compared with results previously reported in the literature [40,41].

2. Experiment

The SiN coatings were produced in a commercial RF planar parallel-plate reactor (Plasmalab µ80, from Plasma Technology) operating at 13.56 MHz. The reactor consists of a base grounded plate connected to the heater, and the upper plate connected to the RF power supply. The system is isolated within a cylindrical Pyrex chamber (see figure 1).

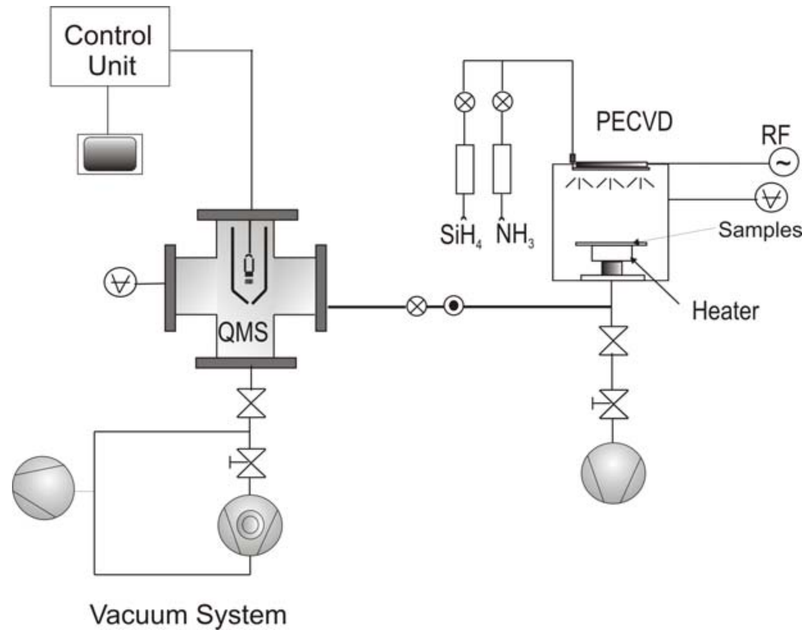

Figure 1. Experimental set-up. Connections between the commercial PECVD system and the Quadrupole Mass Spectrometer (QMS) chamber are shown.

SiH_4 and NH_3 were used as precursors (SiH_4 (99.994%); NH_3 (99.999%), both from Air Product*s*). They were supplied to the reactor through two automatic gas flow valves. A vacuum valve at the reactor's output, in series with a rotary pump, regulated the gas exit. The samples were located on a wafer-plate with temperature control from 20 to 400 ºC, and were maintained at 300 ºC in all the cases. Increasing this temperature would render a reduction of the SiN film hydrogen content [3]; nevertheless, when applied to passivate AlGaN/GaN HEMT, the use of

higher substrate temperatures could damage the metal based Schottky gate contacts previously done [42].

Plasmas were characterized by mass spectrometry. A Stanford Research System quadrupole mass spectrometer (SRS-RGA100) with a Faraday cup as a detector was employed. It was located in a vacuum chamber differentially pumped up to 10^{-4} Pa by a turbomolecular pump and a rotary pump. Since no extra vacuum ports in the commercial PECVD reactor other than its gas output were available, the mass spectrometer system was connected to this point, before the gas exit valve of the reactor, through a vacuum "tee" piece. The gas sampling flow to the spectrometer's chamber was controlled by means of a fine needle valve (in series with a ball valve). Pressure ~ $2 \cdot 10^{-3}$ Pa was maintained in this chamber during the characterization of the plasma.

The refractive indexes and growth rates of the films deposited by PECVD were subsequently analysed by ellipsometry with a PlasMos 2302 equipment, based on a He-Ne laser (λ = 632.8 nm, 45º incident angle). A Fourier Transform Infrared (FTIR) Spectrometer Nicolet Magna IR 760 working in the range 400 – 4000 cm^{-1}, by using a EverGlo IR source, a KBr beamsplitter and a MCT detector cooled with liquid nitrogen, allowed estimating the amplitudes of the Si-H and N-H stretching bands and inferring the hydrogen content in the SiN films. The HEMT devices passivated with these films were characterized by DC and pulsed I–V measurements (gate pulsewidth of 500 μs and a period of 10 ms) by using an Agilent 4156c semiconductor parameter analyzer.

3. Experimental results and discussion

3.a Characterization of the plasma

Figure 2 shows the two mass spectra of the mixed NH_3 and SiH_4 precursors in the reactor, with discharge off and with discharge on in the steady state. In this figure, the RF power was P_{RF} = 30 W and the gas flow rates, 3.1 sccm and 1.7 sccm, respectively. The background spectrum was subtracted previously. The three panels display the regions of interest. Note the different scales in the intensity of the signals (vertical axis) of the left panel and the other ones, which is due, not only to the efficient production of H_2 as major stable product of the discharge, but also to the higher detection efficiency at low masses, commonly found in quadrupole mass spectrometers [34,43]. In what follows, only relative variations of signal intensities are taken into account and, hence, the diverse efficiencies for the various species are not significant. In the middle and right panels of figure 2, bars indicate the characteristic dissociative ionization patterns by electron collisions of NH_3 and SiH_4 [44]. They fit very well the relative intensities of the corresponding peaks of the spectrum without discharge, except for a slightly exceeding signal at 28 a.m.u. This difference at 28 a.m.u, as well as the peak observed with discharge off at 2 a.m.u, where the fragmentation patterns of NH_3 and SiH_4 do not predict any signal; suggest

that some quantities of H_2 and N_2 might be generated by dissociative ionization and subsequent recombination of the precursors in the ionization region of the quadrupole. Similar effects have been reported previously in the literature (see for example [34]).

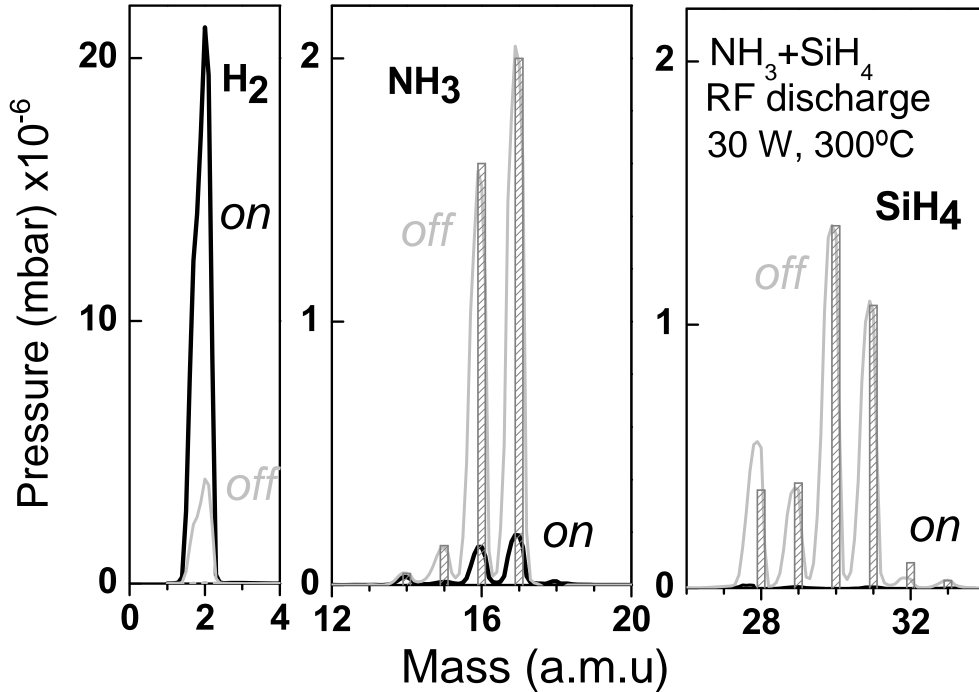

Figure 2. Mass spectra of the mixed precursors for SiN coating without discharge (grey line) and with a 30 W RF discharge (black line). Substrate temperature = 300 ºC. Reactor pressure = 0.7 mbar, $\Phi NH_3/\Phi SiH_4$ = 1.8. The typical dissociation patterns of NH_3 and SiH_4 are shown (bars).

With discharge on, H_2 was generated as major gas product, only a small proportion of ammonia (~10%) remained in the plasma, leading to the corresponding disappearance of the above mentioned contribution to m = 28 a.m.u signal in the quadrupole, and silane was almost completely dissociated (remaining SiH_4 ~ 1%), even for the low RF power applied in this case, leading to the deposition process. As it has been previously commented, and according to bibliographic results [3,26], the N and Si species liberated from the precursors' dissociation are generally assumed to be deposited in the walls by processes involving species such as disilane, at relatively low discharge powers, or $Si(NH_2)_4$ and $Si(NH_2)_3$ radicals, at the higher ones.

In a first series of measurements, the SiN films were deposited on silicon samples at different $\Phi NH_3/\Phi SiH_4$ values from 0.9 to 3, with ΦSiH_4 = 1.7 sccm and P_{RF} = 60 W. In this case, the reactor pressures changed between 88 and 236 Pa, respectively. From the subsequent characterization of the films, $\Phi NH_3/\Phi SiH_4$ = 1.8 was selected as the most appropriate for the

deposition conditions (see below).

In a second series of measurements, the RF power was varied between 30 and 250 W, for $\Phi NH_3/\Phi SiH_4$ = 1.8 (ΦSiH_4 = 1.7 sccm). A total pressure of 70 Pa was maintained in this case. At these conditions, SiN films were grown independently on silicon samples and, finally, on AlGaN/GaN HEMT. Plasma exposures were determined, either by fixing the deposition time (15 min) when applied to silicon substrates, or the desired final film thickness (120 nm), when applied on HEMT. In the last case, the required deposition times to obtain this thickness were previously estimated from the growth rate obtained on Si substrates for each condition.

In figures 3(a) and 3(b), the remaining NH_3 and SiH_4 fractions, and the signals corresponding to H_2 and N_2 produced in the plasma for the different $\Phi NH_3/\Phi SiH_4$ values at P_{RF} = 60 W are depicted. The remaining fractions of NH_3 and SiH_4 were estimated from the intensities ratio between discharge on (in the steady state) and discharge off, for 16 and 31 a.m.u, respectively. At these masses, the background contributions were lower than at the other representative masses of the fragmentation patterns, minimizing possible errors. Linearity of the mass spectrometer was tested from its response to the different NH_3 gas flows without discharge. As can be seen, the remaining fraction of SiH_4 was very small and nearly constant, and neat increases with $\Phi NH_3/\Phi SiH_4$ in the remaining NH_3 fraction and in the H_2 and N_2 signals was appreciated, as could be expected from the gradual excess in NH_3 precursor.

Figures 3(c) and 3(d) show the remaining NH_3 and SiH_4 fractions, and the signals of H_2 and N_2 produced in the plasma, for different RF discharge powers, at $\Phi NH_3/\Phi SiH_4$ = 1.8, during film depositions on HEMT. Between 30 and 125 W, the dissociation of both precursors increased with power, but afterwards, their concentrations clearly stabilized. In all cases, the remaining fraction of NH_3 was noticeably higher than that of SiH_4. The increase in H_2 and N_2 signal with P_{RF} was quite small. The results were very similar (under experimental errors) when the SiN films were deposited on Si substrates. They are not displayed for the sake of simplicity.

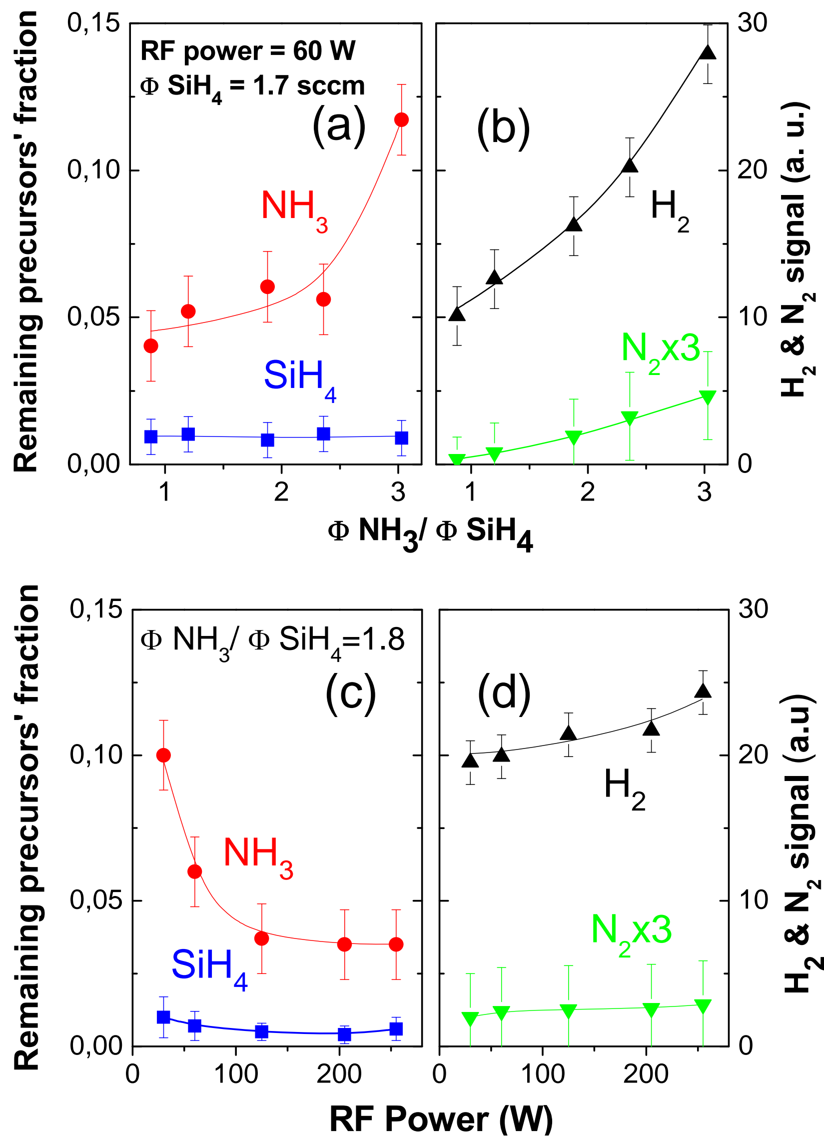

Figure 3. (a) Remaining fractions of SiN precursors, and (b) signals of H_2 and N_2 produced in the steady state discharge, as a function of the NH_3/SiH_4 gas flow ratios. Lines are only to guide the eyes. (c,d) The same data as a function of the applied RF power. N_2 signals in (b) and (c) are magnified by factor 3.

3.b SiN film properties

The thickness and refractive indexes of the SiN films grown at the different plasma conditions were measured by ellipsometry, after extracting the samples from the plasma reactor. From film thickness and deposition times, the deposition rates were directly estimated. The changes in deposition rate and refractive index of the SiN films as a function of $\Phi NH_3/\Phi SiH_4$ are displayed in figure 4(a). Figure 4(b) displays these changes as a function of the applied RF power. By increasing $\Phi NH_3/\Phi SiH_4$ from 0.9 to 3 (figure 4(a)), the refractive index decreased slightly (note the small spread of the vertical scale at the left axis), whereas the deposition rate

almost duplicated its value. The decrease in refractive index can be an indication that SiN film became more rich in nitrogen [6,41], giving place to an increase in the deposition rate. At the higher range of NH_3/SiH_4 flow ratios, both magnitudes varied more slowly. This may suggest a tendency to saturation in the deposition process with the gradual excess of NH_3 supply. These results were all in agreement with previous literature data [40,41], where similar variations were found. This behaviour, and especially, the evolution of the H content with $\Phi NH_3/\Phi SiH_4$ determined afterwards (see figure 6(a)), led us to select an intermediate value, $\Phi NH_3/\Phi SiH_4 =$ 1.8, for the studies at diverse P_{RF} values.

As P_{RF} increased, at $\Phi NH_3/\Phi SiH_4$ = 1.8 (figure 4(b)), the deposition rate multiplied its value by two, and the refractive index increased slightly, until both magnitudes reached a tendency to saturation. These dependences were also in agreement with the results of references [1,40].

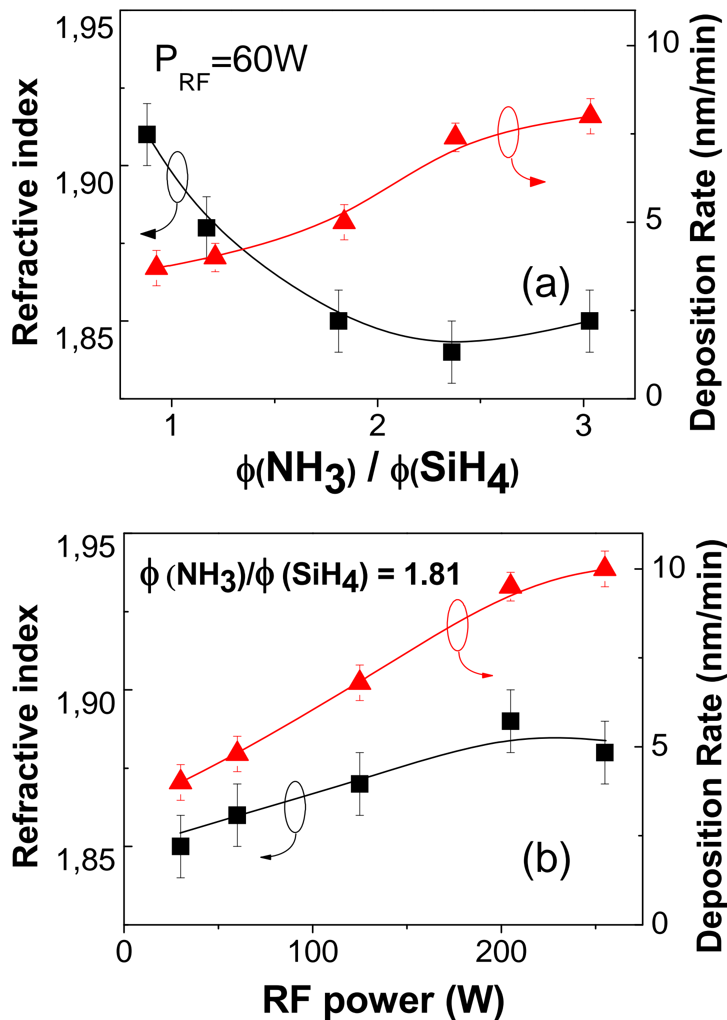

Figure 4. (a) Influence of $\Phi NH_3/\Phi SiH_4$ on the refractive index (left axis) and the deposition rate (right axis) of the SiN films. (b) The same, as a function of P_{RF}.

It is worth mentioning that the tendencies to stabilization in refractive index and deposition rate with increasing $\Phi NH_3/\Phi SiH_4$ shown in figure 4(a) can be related with a clear growth in the NH_3 excess observed in the mass spectrometric data (see figure 3(a)). Conversely, the tendency to stabilization in refractive index and deposition rate with increasing P_{RF} displayed in figure 4(b) coincides with the fact that, at the higher P_{RF} values, the dissociation efficiency of the precursors do not increase further (figure 3(c)).

The effects of $\Phi NH_3/\Phi SiH_4$ and P_{RF} variations on the hydrogen content in the SiN films were determined from the intensities of the infrared Si-H and N-H stretching bands in spectra measured by Fourier Transform Infrared Spectroscopy [40,45] like the one drawn in figure 5.

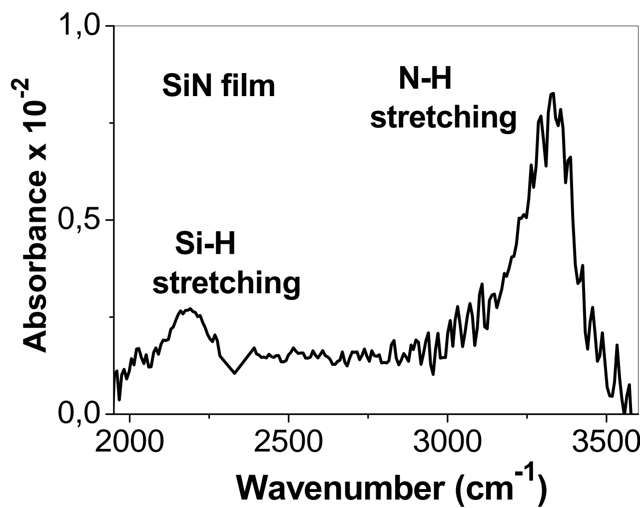

Figure 5. Infrared spectrum of a SiN film deposited under $\Phi NH_3/\Phi SiH_4 \sim 1.8$ and $P_{RF} = 200$ W conditions.

According to the literature [6,45], low H concentrations in the SiN films are highly convenient and determinant of their passivation properties in HEMT. Figure 6 displays the decreases in H content of the SiN films by increasing $\Phi NH_3/\Phi SiH_4$ (a) and RF power (b), up to reaching minimum stationary values for $\Phi NH_3/\Phi SiH_4 \sim 1.8$ and $P_{RF} \sim 125$ W, respectively. The initial decrease in H content was remarkably greater for the case of $\Phi NH_3/\Phi SiH_4$ variation than that registered by changing P_{RF}. In any case, the regions of minimum stationary H content in the films correspond in both cases to the higher H_2 gas concentrations observed in the plasma (see figure 3(b) and 3(d)). Moreover, concerning P_{RF}, the minimum H content also corresponds to the region where the dissociation degrees of NH_3 and SiH_4 reached the steady state (figure 3(c)). These results deserve also to be compared to the intervals of $\Phi NH_3/\Phi SiH_4$ and P_{RF} values where some tendencies to saturation were found in the refractive index and deposition rate of

the films (figure 4(a,b)), and are in agreement with the observations reported in references [1,45].

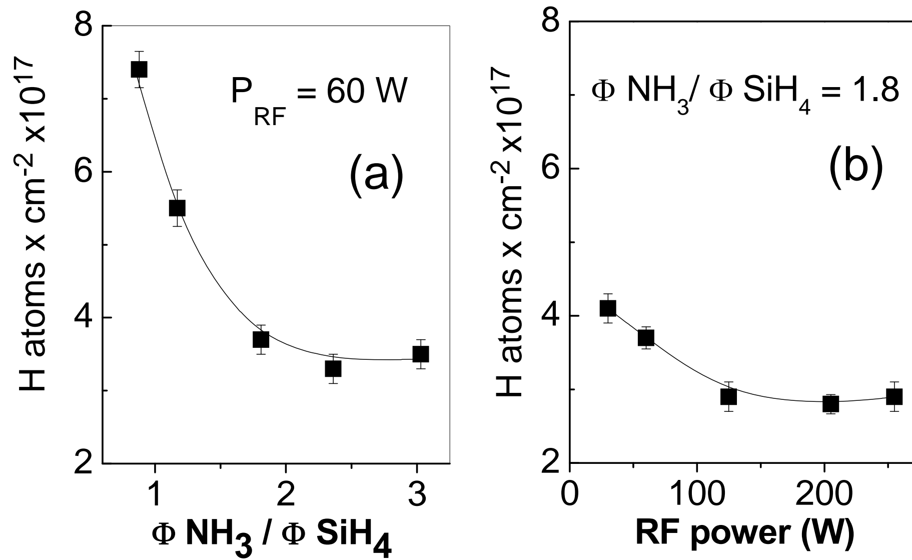

Figure 6. (a) Variation of H content (atoms per surface unit) in the SiN films as a function of $\Phi NH_3/\Phi SiH_4$ for P_{RF} = 60 W. (b) Variation of the H content with the RF power for reactor pressure = 0.7 mbar and $\Phi NH_3/\Phi SiH_4$ = 1.8. The film thickness was 120 nm.

3.c Characterization of HEMT

Figure 7 illustrates schematically a HEMT device with (upper panel) and without (lower panel) conduction, depending on the potential applied to the gate, G, being D the drain and S, the source of the transistor.

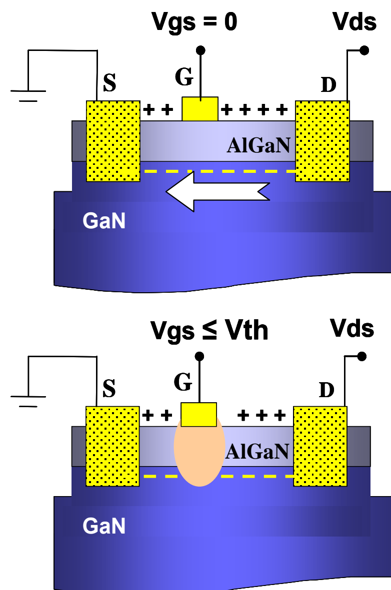

Figure 7. Scheme of the AlGaN/GaN HEMT devices working at open channel (V_{GS} = 0V) (up) and without conduction (below a threshold V_{GS} potential) (down).

The output characteristics of HEMT passivated with SiN, to DC and pulses of 500 µs, were measured using the semiconductor parameter analyzer previously mentioned. The results for two HEMT passivated at different plasma P_{RF} values are shown in figure 8. Slight hysteresis phenomena, usually related to the presence of trapped charges in the device, are especially appreciable in the case of the devices passivated using the lowest P_{RF} values (30 W) (see circles in figure 8).

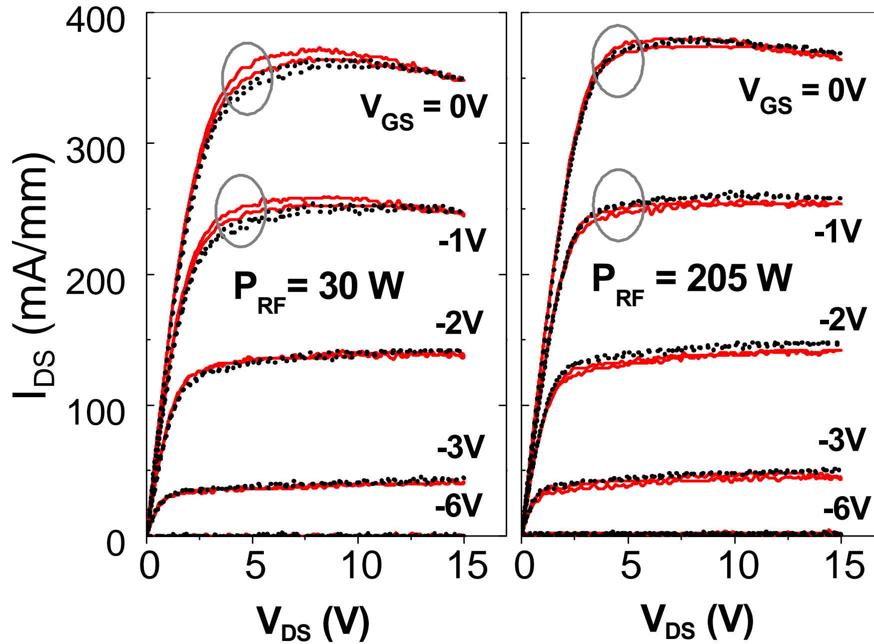

Figure 8. Output characteristic of AlGaN/GaN HEMT for DC (continuous lines) and pulsed signals (dashed lines), after pasivation with SiN films deposited at 30 W (left) and 205 W (right).

To further investigate the influence of P_{RF} during SiN film deposition in the trapping of charges, the effect of current collapse, defined as I_{DS}(DC)/I_{DS}(pulsed) at V_{DS}=5 V, was estimated from the output characteristic at V_{GS}= 0V (see figure 8) for the different P_{RF} values. Although a 500µs pulse width was quite long to extract the current collapse, which affects most of this kind of devices for radiofrequency applications, it was short enough to allow an estimation of the quality of the device at moderate high frequencies. The results displayed in figure 9 indicate that current collapse is reduced when high P_{RF} are applied to the plasma during SiN deposition, implying a reduction of slow trapped charges that degrade the electrical behaviour of this kind of devices [46,47]. This is in good agreement to previous results [40] and shows that SiN films with a lower H content are more effective to mitigate current collapse effects.

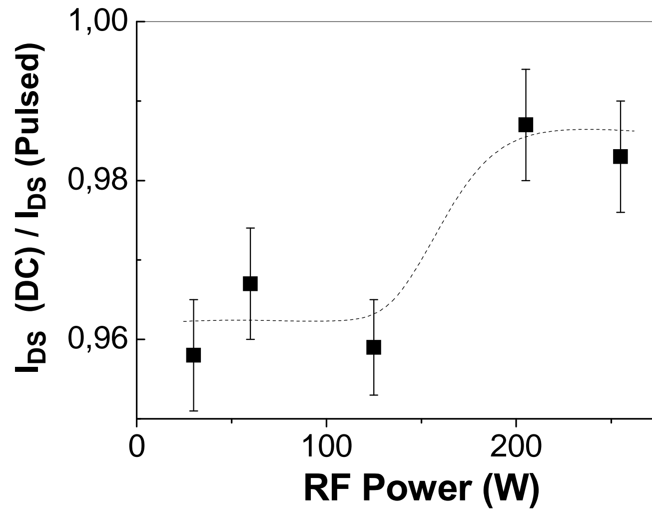

Figure 9. Variation of the ratio I_{DS}(DC)/I_{DS}(pulsed) on AlGaN/GaN HEMT with the RF power applied to the plasmas during SiN deposition. The higher proximity of this value to unity for the higher P_{RF} values indicates a lower current collapse.

On the other hand, the maximum drain-source currents ($I_{DS\ max}$), estimated from characteristic curves like those of figure 8, as a function of P_{RF}, are depicted in figure 10. A noticeable increase in the $I_{DS\ max}$ was obtained for P_{RF} =200 W, as compared to the values at the lowest P_{RF} values. In this region of higher P_{RF} values, saturation in the I_{DS} maximum was observed, in accordance with the regions of saturation behaviour obtained for the precursors' dissociation and the other magnitudes studied in this work.

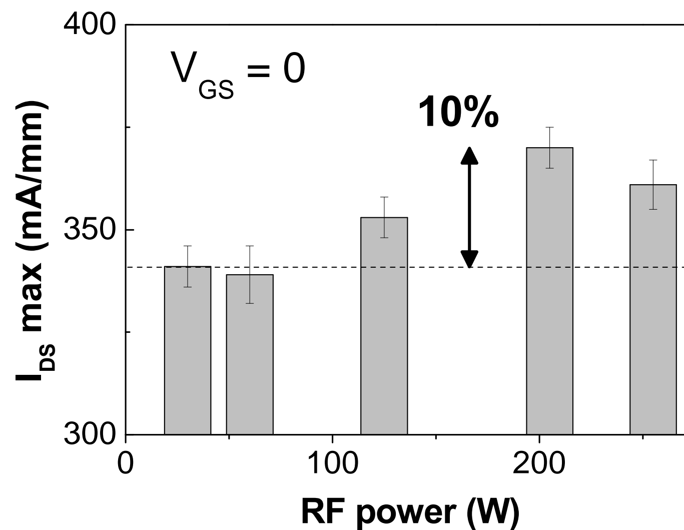

Figure 10. Influence of P_{RF} during SiN film deposition on the maximum drain-source currents obtained for HEMT, estimated from their characteristic curves.

4. Summary and conclusions

In this work, the composition of plasmas generated in a commercial RF discharge reactor containing NH_3 and SiH_4 for PECVD of SiN films was studied by mass spectrometry, as a function of the NH_3/SiH_4 flow ratios and the RF power applied to the reactor. The SiN films were grown on silicon samples and, as passivating coatings, on high electron mobility transistors. The properties of the films and of the HEMT were studied afterwards by different complementary techniques.

The dissociation degree of the precursors and the concentration of H_2 and N_2 produced in the plasma were related to the deposition rate and refractive index of the films, and, fundamentally, to their H content and to the electric response of the passivated transistors.

The studies varying $\Phi NH_3/\Phi SiH_4$ allowed selecting an intermediate value for this magnitude, where the H content of the films got minimum values and stabilized. Besides, at higher $\Phi NH_3/\Phi SiH_4$ than this value (1.8), NH_3 was in excess, and its dissociation efficiency decreased noticeably, whereas the H_2 (and N_2) gas content in the plasma increased markedly.

The studies varying P_{RF} demonstrated that the H content of the SiN films decreased further with growing RF power, and reached minimum stationary values for P_{RF} higher than 125 W, corresponding to minimum and stationary remaining concentrations of the precursors. The decrease in the H film content and in the remaining plasma precursors coincided too with the improvement of the HEMT electrical characteristics.

These results confirm that the NH_3/SiH_4 gas flow ratio and the RF power are critical values during SiN film deposition for the effective passivation of AlGaN/GaN HEMT, in agreement with previous literature data. These results also suggest that the properties of the film and the passivated HEMT are closely related with the dissociation efficiency of the precursors in the depositing plasmas, and their H_2 content. So, efforts for *in-situ* characterization of the plasma during the depositing process in commercial reactors like the one employed here can guide encountering the best film growth conditions, saving great time and effort in finding these conditions by later *ex-situ* characterization of the devices.

Aknowledgements

This work was supported in part by the KORRIGAN project (EDA—04/102.052/032 CA 2157v7) and in part by the projects ICTS-2007-05, MAT2007-65965, FIS 2007-61686 and CSD2009-00038 of the MICINN of Spain.

References:

[1] Smith DL, Alimonda AS, Chen CC, Ready SE, Wacker B 1990 *J. Electrochem. Soc.* **137** 614

[2] Smith DL, Alimonda AS, Vonpreissig FJ 1990 *J. Vacuum Sci. Tech. B* **8** 551

[3] Smith DL, Alimonda AS, Chen CC, Tuan H C 1990 *J. Electronic Mater.* **19** 19

[4] Murata T, Kono K, Tsunemine Y, Fujisawa M, Matsuura M, Asai K, Koilma M 2008 *Japanese J. App. Phys.* **47** 2488

[5] Ma T P 1998 *IEEE Trans. Electron Devices* **45** 680

[6] Flewitt A J, Dyson A P, Robertson J, Milne W I 2001 *Thin Solid Films* **383** 172

[7] Kessels W M M, van den Oever P J, Bosch R C M, Bijker M D, Evers M, Schram D C, van de Sanden M C M 2005 *High Technol. Plasma Processes* **9** 141

[8] Duerinckx F, Szlufcik J 2002 *Solar Energy Mater. Solar Cells* **72** 231

[9] Cianci E, Schina A, Minotti A, Quaresima S, Foglietti V 2006 *Sens. Actuators* A **127** 80

[10] Onojima N, Higashiwaki M, Suda J, Kimoto T, Mimura T, Matsui T 2007 *J. Appl. Phys.* **101** 043703

[11] Mishra U K, Shen L, Kazior T E, Yi-Feng W 2008 *Proc. IEEE* **96**, 287

[12] Cuerdo R, Calle F, Braña A F, Cordier Y, Azize M, Baron N, Chenot S, Muñoz E 2008 *Phys. Stat. Sol. C* **5** 1971.

[13] Cuerdo R, Sillero E, Romero M F, Uren M J, di Forte Poisson M A, Muñoz E, Calle F 2009 *IEEE Electron Dev. Let.* **30** 808

[14] Dongfang W, Xiaojuan C, and Xinyu L. 2010 *J. Semicond.* **31**, 024001.

[15] Manasreh M O 1997 *Optoelectronic Properties of Semiconductors and Superlattices*, Vol. 2. New York: Gordon and Breach

[16] Hasegawa H 2007 *Curr. Appl. Phys.* **7** 318

[17] González-Posada Flores F, Rivera C, Muñoz E 2009 *Appl. Phys. Lett.* **95** 203504

[18] Romero M F, Jiménez A, Miguel-Sánchez J, Braña A F, González-Posada F, Cuerdo R, Calle F, Muñoz E 2008 *IEEE Electron Dev. Lett.* **29** 209

[19] Gordillo-Vazquez F J, Albella J M 2004 *Plasma Sources Sci. Technol.* **13** 50

[20] Gordillo-Vázquez F J, Herrero V J, Tanarro I 2007 *Chemical Vapor Deposition* **13** 267

[21] Sanz M M, Tanarro I 2008 *"Plasmas basic concepts and nitrogen containing plasmas"* in *"Nitrides and dilute nitrides: Growth, physics and devices"* pp 15-46. Ed. J. Miguel-Sánchez, Transworld Research, Kerala, India, ISBN: 81-7895-250-5

[22] Gordillo-Vazquez F J, Camero M, Gomez-Aleixandre C 2006 Plasma Sources Sci. Technol. **15** 42

[23] Lopez-Santos C, Yubero F, Cotrino J, Contreras L, Barranco A, Gonzalez-Elipe A R 2009 *Plasma Proc. and Polymers* **6** 555

[24] Gomez-Aleixandre C, Sanchez O, Castro A, Albella J M 1993 *J. Appl. Phys.* **74** 3752

[25] Castillo M, Herrero V J, Méndez I, Tanarro I 2004 *Plasma Sources Sci. Technol.* **13** 343

[26] Kessels W M M, van Assche F J H, van den Oever P J, van de Sanden M C M 2004 *J. Non-Crystalline Solids* **338–340** 37

[27] van den Oever P J, van Helden J H, van Hemmen J L, Engeln R, Schram D C, van de Sanden M C M, Kessels W M M 2006 *J. Appl. Phys.* **100** 093303

[28] Ropcke J, Welzel S, Lang N, Hempel F, Gatilova L, Guaitella O, Rousseau A, Davies P B 2008 *Appl. Phys. B-Lasers and Optics* **92** 335

[29] de los Arcos T, Domingo C, Herrero V J, Sanz M M, Schulz A, Tanarro I 1998 *J. Phys. Chem. A* **102** 6282

[30] Tanarro I, de los Arcos T, Domingo C, Herrero V J, Sanz M M 2002 *Vacuum* **64** 457

[31] Sanz M M, Abad L, Herrero V J, Tanarro I 1992 *J.Appl.Phys.***71** 5372

[32] Tabarés F L, Tafalla D, Tanarro I, Herrero V J, Islyaikin A M 2004 *Vacuum* **73** 161

[33] Ohta H, Nagashima A, Hori M, Goto T 2001 *J. Appl. Phys.* **89** 5083

[34] Tanarro I, Herrero V J, Islyaikin A M, Méndez I, Tabarés F L, Tafalla D 2007 *J. Phys. Chem. A* **111** 9003

[35] Tanarro I, Herrero V J 2009 *Plasma Sources Sci. Technol.* **18** 034007

[36] Rousseau A, Teboul E, Lang N, Hannemann M, Ropcke J 2002 *J. Appl. Phys.* **92** 3463

[37] Castillo M, Herrero V J, Tanarro I 2002 *Plasma Sources Sci. Technol.* **11** 368

[38] Lang N, Ropcke J, Wege S, Steinbach A 2010 *European Phys. J-Appl. Phys.* **49** 13110

[39] Tanarro I, Sanz M M, Romero M F, Muñoz E, Jiménez A *19th International Symposium on Plasma Chemistry* (ISPC). Bochum, Germany, 26-31 July 2009

[40] M.C.J.C.M. Krämer 2006 "*Gallium nitride-based microwave high-power heterostructure field-effect transistors design, technology and characterization*". PhD Thesis, Eindhoven Technische Universiteit, ISBN-13: 978-90-386-1893-7

[41] B. Kim, D.W. Kim, S.S. Han, 2004 *Vacuum*, **72**, 385

[42] Monroy E, Calle F, Ranchal R, Palacios T, Verdú M, Sánchez F J, Montojo M T, Eickhoff M, Omnès F, Bougrioua Z, Moerman I. 2002 *Semicond. Sci. Technol.* **17**, L47

[43] Méndez I, Herrero V J, Tanarro I 2010 *Phys. Chem. Chem. Phys.* **12** 4239

[44] http://webbook.nist.gov/chemistry/form-ser.html

[45] Lanford W A, Rand M J 1978 *J. Appl. Phys.* **49**, 2473

[46] Klein P B, Binari S C, Ikossi K, Wickenden A E, Koleske D D, Henry R L 2001 *Appl. Phys. Lett.* **79**, 3527

[47] Klein P B, Binari S C, Ikossi-Anastasiou K, Wickenden A E, Koleske D D, Henry R L, Katzer D S 2001 *Electron. Lett.*, **37**, 661